An off center quadrupole acoustic wireline tool: numerical modeling and field data analysis

Zhou-tuo Wei, COSL-UPC Allied Borehole Acoustic Lab., China University of Petroleum (UPC); Hua Wang, Earth Resources Lab., Massachusetts Institute of Technology and CUPB; Xiao-ming Tang, COSL-UPC Allied Borehole Acoustic Lab.in UPC; Meng Li, CPUB*

Summary

The complex wavefield makes the velocity determination difficult when the tool is off center or tilted. We use the discrete wave number integration, slowness-time-semblance (STC), and dispersion analysis methods to investigate the wavefield acquired by an off center wireline quadrupole tool. We analyze the extraction of shear wave (S-wave) velocity in both the soft and fast formations. Then, we use the field data examples acquired by the off center quadrupole tool to demonstrate the validity and capability of the theoretical analysis and data processing method.
It is shown that the amplitude of leaky-P wave in the slow formation increases significantly in the off center tool case compared to the centralized tool case. The leaky-P wave and noise can be suppressed according to the distribution in the STC at different wavelet scales. The dipole mode has a dominant contribution to the synthetic waveforms in both slow and fast formations when the quadrupole tool is off center. According the features of the data, we propose a data processing flow to get the S-wave velocity from the wavefield acquired by the off center quadrupole wireline tool. For the slow formations, we use a high band-pass filter to get the quadrupole component and then a dispersion method to determine the S-wave velocity after the leaky-P wave and noise being removed. However, for the fast formations, we use a low band-pass filter and a waveform inversion with a short time window to get the dipole component, and then the dispersion method to get the S-wave velocity.

Introduction

S-wave velocity is an important parameter for the porosity and saturation determinations, fracture detection. Researchers pay attentions to the wave propagation and the extraction of S-wave velocity from acoustic logs. The wave propagation is complicated if the tool is off center or tilted (e.g. Wang et al., 2013, 2015). In addition, due to the influence of source frequency, borehole and formation properties, the field data sets are often mixed with additional modes and noises comparing with the ideal logging environments (e.g. Tang and Cheng, 2004), which challenges the velocity determination and data analysis.

Willis et al. (1982) evaluated the approximate effects of the off center and/or tilted tool by using an effective borehole radii and ray tracing method. The multipole wavefields excited by the eccentric sources (Leslie et al., 1990; Schmitt, 1993; Randal, 1991) have also been investigated.Zhang (1996) investigated the non-axisymmetric acoustic fields excited by a tool off the borehole axis. Byun and Toksöz (2006) investigated the effects of an off center tool on the multipole waveforms. Wang et al. (2013, 2015) studied the wavefields of the off center acoustic mulitipole logging-while-drilling (LWD) tool. As an optional for S-wave velocity determination, qudarupole tool has been commercially successful in the LWD. However, it is studied very few in the wireline because the S-wave velocity determination got from dipole tool are considered effective enough. Unfortunately, the previous studies in wireline tool imply the S-wave velocity cannot get correctly when the monopole and dipole tools are off center. Therefore, it still requires study on the wavefield generated by an off center quadrupole wireline tool to determine the S-wave velocity.

In this study, we investigate the synthetic wavefields generated by the off center quadrupole wireline tool. The numerical results of the full waveforms and the dispersion are provided to help us analyze the wavefield and S-wave velocity determination in the off center tool case in both soft and fast formations. Finally, we use the proposed method to process the field data acquired by the off center quadrupole wireline tool.

Models and Parameters

Figure 1 shows the off center quadrupole tool in the fluid-filled boreholes. A, B, C, and D are the positions of the source-receiver arrays. In the following discussion, XA, XB, XC and XD denote the response of A, B, C and D positions. The elastic parameters and geometries of the model used in the simulations are listed in Table 1.

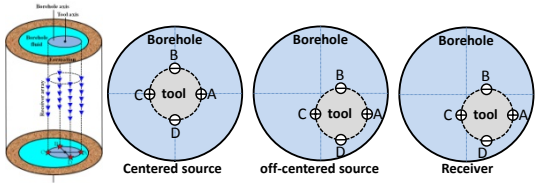

Figure 1. Schematic diagram for the off center quadrupole wireline tool in fluid-filled borehole. (a) Receivers arrays are on the same planes with the source components A, B, C, and D, (b) The configuration of the source assembly in the centralized case, (c) The top-down view of the source, (d) Rceiver array in the off-centered 45° case, respectively.

Numerical simulation and results analysis

We only discuss the off center tool with the tool paralleling to the borehole axis. In the off center cases, the receivers are moved as the same direction as the source with a radial

offset of 4.064 cm with an angle of 45° (as shown in Figures 1c and 1d). We use a Ricker wavelet with a center frequency of 4.0 kHz as the source function. The quadrupole source is loaded by four point sources: A, B, C, and D with alternative phases as shown in Figures 1b and 1c.

Table 1. Model parameters used in the simulations

Medium	V_p (m/s)	V_s (m/s)	Density (g/cm^3)	Radius (mm)
Borehole mud	1600	—	1.00	101.6
Fast formation	4200	2700	2.15	∞
Slow formation	1900	950	2.00	∞

1. Wavefield analysis for the off center tool with the angle of 45° in soft formation

Figure 2 shows the synthetic waveforms of XA at the spacing of 1.5 m in the slow formation for the centralized and off center cases. Using a discrete wavenumber integration method, we can get not only the full waveform but the contributions of different modes for the full waveform, such as monopole (n = 0), dipole (n = 1), quadrupole (n = 2), hexapole (n = 3) modes and more modes (e.g. Byun and Toksöz, 2006; Chen et al., 2009). We consider the n = 0 to n = 18 in the full waveform calculation. The contributions of the monopole, dipole, quadrupole and hexapole modes are also shown in Figures 2a and 2b because the contributions of higher modes can be ignored nearly. The corresponding dispersion curves of the array waveforms are got from the weighted spectral semblance with a Gaussian function (WSS) (Tang and Cheng, 2004) (as shown in Figures 2c and 2d).

From Figure 2a, it is clear to find the amplitude of the synthetic waveform is roughly equal to the quadrupole mode (n=2) and the contributions from other modes are zero when the tool is centralized. The first arrival around 0.75 ms is leaky-P wave (Tang and Cheng, 2004) as shown in the black box of Figure 2a. The waveform is amplified by 100 times for identification. The second arrival around 1.40 ms is the quadrupole mode.

The waveform is different from that in the centralized tool when the quadrupole tool is off center (Figure 2b). The leaky-P wave with a significant amplitude (as highlighted by the left rectangular in Figure 2b) advances with the arrival of 0.65 ms. In addition, the quadrupole mode at about 1.35 ms is contaminated by other modes. The dipole mode exhibits the greatest amplitude. Amplitudes of other modes in the sequence from large to small are the quadrupole, hexapole and monopole modes. The increasing eccentricity destroys the excitation of quadrupole source, which induces the nearby positive and negative sources as a dipole vibration under the limit of the borehole. We can easy to find the amplitude of quadrupole mode decreases with the tool eccentricity increasing, while it is a completely opposite trend for the dipole mode. Figure 2c and Figure 2d give the dispersion curves of array waveforms in XA with the spacing from 0.9m to 1.8m and receiver interval of 0.1m.

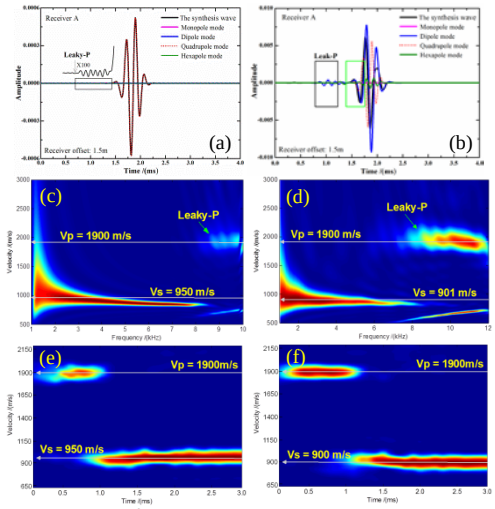

Figure 2. The waveforms, the semblance plots and the dispersion images of the quadrupole responses in the slow formation. (a) The waveform of XA for an centralized quadrupole wireine tool and (b) an off center 45° quadrupole wireine tool; (c) The dispersion for (a); (d) The dispersion for (b); (e) The STC for (a); (f) The STC for (b).

Compare the Figure 2c and 2d, we can find the dispersion of leaky-P wave is still weak when the quadrupole tool is off center, but the coherence becomes stronger than that in the tool centralized case. By the STC, we can easily get the P-wave velocity (as shown in Figure 2e and Figure 2f), which are in good agreement with the P-wave velocity of the model. We also get the S-wave velocity from the dispersion in Figure 2c when the tool is centralized. However, the S-wave velocity (about 900 m/s) got from the dispersion (Figure 2d) and STC methods (Figure 2f) are less the model velocity. It is imply the S velocity determination is damaged when the tool is off center.

In addition, the Leaky-P wave with increasing amplitude also shows an adverse effect on the extraction of S-wave velocity. Although the disturbance could be alleviated by choosing an appropriate time window during the STC processing, leaky-P wave in field data usually has a long trail making it hard to determine the truncate time window. In order to suppress leaky-P wave and other noise signal, we employ a dual-tree complex wavelet transform method (DTCWT) combined with STC to decompose the signal into multiple time-frequency domains (Li et al., 2014). Using the array waveforms in XA as the input signal, the corresponding STC plots of wavelet components at each scale are obtained as shown in Figure 3. The SNR of the level 5 is higher than the original waveform. Then, we use

a regional threshold to wipe off the wavelet coefficients of the leaky-P wave according to the distribution in the STC plot at each level. Using the processed wavelet coefficients, we reconstruct the waveform (as shown in Figure 4a), where the leaky-P wave has been substantially suppressed.

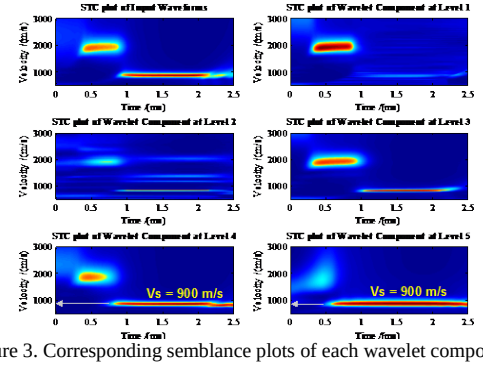

Figure 3. Corresponding semblance plots of each wavelet component.

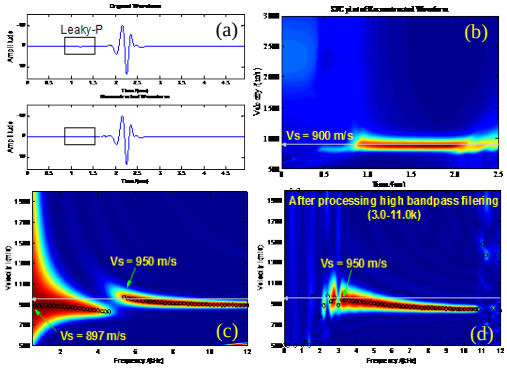

Figure 4. (a) Comparison of waveforms before and after leaky-P wave suppressed in the off center case; (b) and (c) are the STC and dispersion after data with leaky-P wave being removed; (d) Dispersion for the reconstructed data after high band-pass filtering.

Figures 4b and 4c show the STC and dispersion of reconstructed array waveforms, respectively. We can find the main contributions of synthetic waveforms are dipole and quadrupole modes with the velocities of 897 m/s and 950 m/s at the cutoff frequency. After a high band-pass filtering, the dispersion of the reconstructed data is shown in Figure 4d. We can get the right S-wave velocity from the dispersion of the remained quadrupole mode.

2. Wavefield analysis for the off center tool with the angle of 45° in fast formation

Figure 5 shows the synthetic full waveforms and the corresponding four modes at XA at the spacing of 1.5 m in a fast formation for an centralized quadrupole tool (Figure 5a) and the off center tool with an angle of 45° (Figure 5c), and dispersion curves (Figure 5b for Figure 5(a), Figure 5d for Figure 5(c)).

In the centralized case, the amplitude of full waveform is roughly equal to the quadrupole mode, and the contributions from other modes are zero. However, for the off center tool case (Figure 5c), the quadrupole mode is contaminated by other modes. The dipole mode is dominant completely, which has same phase as the quadrupole mode in the first 2-3 cycles of the waveform. Therefore it is easy to get the S-wave velocity by using STC or other frequency domain methods.

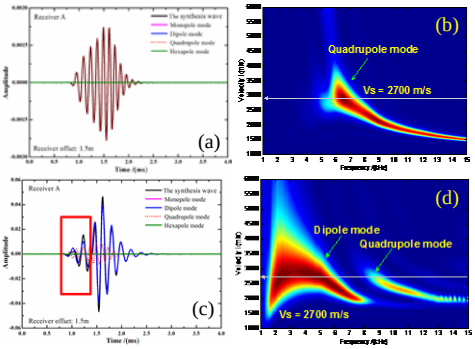

Figure 5. The waveforms, and the dispersion curves of the quadrupole tool responses in the fast formation. (a) The waveform in the centralized case; (b) The waveform for the tool off center with the angle of 45° ; (c) Dispersion for (a); (d) Dispersion for (c).

Specifically, we can extract the formation S-wave velocity in three steps for the off center quadrupole wireine tool in a fast formation. ① Performing a low band-pass filtering as much as possible to eliminate the influence of quadrupole mode; ② Extracting the arrival time of the first wave based on a waveform inversion method; ③ Short time window processing (As the red box shown in Figure 5c). The time window can be an exponential function.

Field data analysis and processing

We use the theoretical analysis results and data processing methods described above to help us understand the field examples acquired by a quadrupole tool in an open hole. The heavy mud with the velocity of about 1800m/s is used in this field. The tool configuration is similar as Figure 1 and we only use the waveform in the XA receiver here. The array contains four receivers with the spacing ranges from 1.5 m to 2.1 m and receiver interval of 0.2 m.

Case1: Slow formation

DTCWT is first used to suppress the leaky-P wave and noise in the time-frequency domains. Figure 6a and 6b show the wavelet components at each scale (Figure 6a) and the raw waveform (upper left in Figure 6b). It is obvious the SNR of level 5 is higher than the original waveform. Figures 6b and 6c show the comparison between the waveform before and after of leaky-P wave being removed. As shown in black box of Figure 6b, the leaky-P wave is

removed successfully. Figure 6c shows the dispersion by WSS for the reconstructed waveforms and the semblance peak value is difficult to be picked up. Figure 6d shows dispersion analysis of performing a long time window process. It is similar as Figure 4c. After a high band-pass filtering (8.0-12.0 kHz) on the reconstructed data, the dispersion (Figure 6e) has a better performance than that in Figure 6d. Then we can get the S-wave velocity (1540m/s) from the dispersion. It illustrate that the multi-scale analysis is an effective way for suppressing the leaky-P wave and the high band-pass filtering and time window processing can improve the accuracy of S-wave velocity determination.

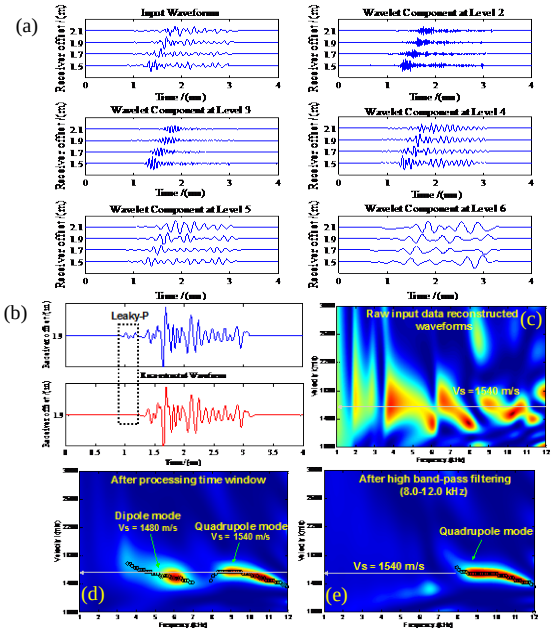

Figure 6. Field data in the slow formation. (a) Wavelet component at each scale; (b) Original and reconstructed waveforms; (c) Dispersion of reconstructed array waveforms; (d) Dispersion of the reconstructed data after a long time window processing; (e) Dispersion of the reconstructed data after the high band-pass filtering and time window processing.

Case2: Fast formation

Figure 7 shows a field data in the fast formation. Figure 7b shows dispersion analysis for the raw data and the semblance peak value is less than 2453m/s. Figure 7c shows the dispersion analysis for the data after low band-pass filtering (2.0-8.0 kHz). It is obvious that the data with a low pass filter has a better performance than that in Figure 7b. Using the waveform inversion technique with an exponential function (Lang, 2014), we perform a short time window processing to determine the first arrival time of the wave. Then the dispersion method is used to help us determine the S-wave velocity as shown in Figure 7c. We find it is very easy to pick up the S-wave velocity (about 2453 m/s).

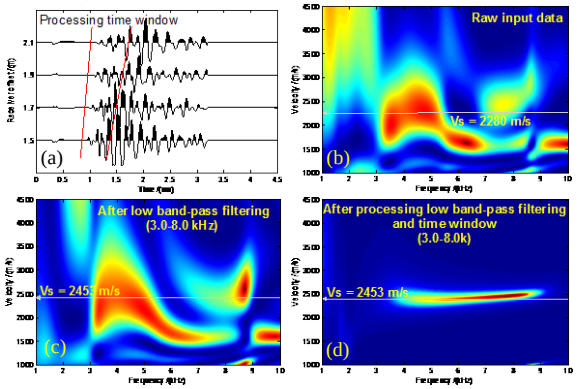

Figure 7. Field data and the dispersion for the fast formation. (a) Field array waveforms; (b) Dispersion for the raw data; (c) Dispersion for the data after low band-pass filtering; (d) Dispersion for the data after low band-pass filtering and time window processing.

Conclusions

In this paper, we use the wave number integration, STC, and dispersion analysis to investigate the wavefields generated by the off center quadrupole tool. Conclusions are summarized as below:

- The amplitude of the leaky-P wave increases significantly when the tool is off center. The leaky-P wave and the noise can be suppressed according to their distribution in semblance at different wavelet scales.
- The dipole mode dominates the synthetic waveforms both in slow and fast formations when the tool is off center.
- S-wave velocity can be extracted from the quadrupole mode by a high band-pass filter when the tool is off center in the slow formation. However, the S-wave velocity in the fast formation can be extracted from the dipole mode by a band-pass filter, a waveform inversion with a time window and velocity analysis in time-frequency domain.

Acknowledgments

The work is supported by the NSFC (Nos. 41404091 and 41404100), Shandong Province NSF (ZR2014DQ004), the Fundamental Research Funds for the Central Universities (15CX02001A), a China Post-doctoral Science Foundation (NO. 2013M530106) and The International Postdoctoral Exchange Fellowship Program.

Reference

Byun J., and M. N. Toksöz, 2006, Effects of an off-centered tool on dipole and quadrupole logging: Geophysics, 71(4), F91–F100.

Chen, T., Wang, B., Zhu, Z., and Burns, D., 2010, Asymmetric source acoustic LWD for improved formation shear velocity estimation: SEG Technical Program Expanded Abstracts, 548–552.

Lang, X. Z., 2014, The study of inversion method about first-arrival time in array waveform: M.S. thesis, China University of Petroleum (East China).

Leslie, H. D., and C. J. Randall, 1990, Eccentric dipole sources in fluid filled borehole: Numerical and experimental results: J. Acoust. Soc. Am., 87, 2405–2421.

Li, M., G. Tao, and H. Wang, et al., 2014, An improved multi-scale analysis for the inversion of shear wave anisotropy with cross-dipole logs: SPWLA 55th Annual Logging Symposium, May 18–22.

Randall, C. J., 1991, Modes of non-circular fluid-filled borehole in elastic formation: J. Acoust. Soc. Am. 89, 1002–1016.

Schmitt, D. P., 1993, Dipole logging in cased borehole: J. Acoust. Soc. Am., 93, 640–657.

Tang, X. M., and C. H. Cheng, 2004, Quantitative Borehole Acoustic Methods. Elsevier, Amsterdam.

Wang, H., G. Tao, and K. Zhang, 2013, Wavefield simulation and analysis with the finite-element method for acoustic logging while drilling in horizontal and deviated wells: Geophysics, 78(6), 525–543.

Wang H., G. Tao, M. C., Fehler, 2015, Investigation of the high-frequency wavefield of an off center monopole acoustic Logging-While-Drilling tool: Geophysics (in press)

Willis, M. E., M. N. Toksöz, and C. H. Cheng, 1982, Approximate effects of off-Center acoustic sondes and elliptic boreholes upon full waveform logs: 52ndAnnual International Meeting, SEG, Expanded Abstracts, 321–322.

Zhang, B., 1996, Nonaxisymmetric acoustic field excited by a cylindrical tool placed off a borehole axis and extraction of shear wave: Journal of the Acoustical Society of America, 99, 682–690.